

# How to assess light trapping structures versus a Lambertian Scatterer for solar cells ?

Christian S Schuster,<sup>1,\*</sup> Angelo Bozzola,<sup>2</sup> Lucio C Andreani,<sup>2</sup> and Thomas F Krauss<sup>1</sup>

<sup>1</sup>Department of Physics, University of York, York, YO10 5DD, UK

<sup>2</sup>Department of Physics, University of Pavia, Via Bassi 6, 27100 Pavia, Italy

\*christian.schuster@york.ac.uk

**Abstract:** We propose a new figure of merit to assess the performance of light trapping nanostructures for solar cells, which we call the light trapping efficiency (LTE). The LTE has a target value of unity to represent the performance of an ideal Lambertian scatterer, although this is not an absolute limit but rather a benchmark value. Since the LTE aims to assess the nanostructure itself, it is, in principle, independent of the material, fabrication method or technology used. We use the LTE to compare numerous proposals in the literature and to identify the most promising light trapping strategies. We find that different types of photonic structures allow approaching the Lambertian limit, which shows that the light trapping problem can be approached from multiple directions. The LTE of theoretical structures significantly exceeds that of experimental structures, which highlights the need for theoretical descriptions to be more comprehensive and to take all relevant electro-optic effects into account.

©2014 Optical Society of America

**OCIS codes:** (040.5350) Photovoltaic; (050.1950) Diffraction gratings; (050.5298) Photonic crystals; (310.6628) Subwavelength structures, nanostructures; (350.4238) Nanophotonics and photonic crystals; (350.6050) Solar energy.

---

## References and links

1. A. Jäger-Waldau, JRC PV Status Report 2013, <http://iet.jrc.ec.europa.eu/remea/pv-status-report-2013>.
2. T. Tiedje, E. Yablonovitch, G. Cody, and B. Brooks, "Limiting efficiency of silicon solar cells," *IEEE Trans. Electron. Dev.* **31**(5), 711–716 (1984).
3. A. Goetzberger, "Optical confinement in thin Si solar cells by diffuse back reflectors," *Proceedings of the 15th IEEE Photovoltaic Specialists Conference*, Orlando, 867–870 (1981).
4. E. Yablonovitch and G. D. Cody, "Intensity enhancement in textured optical sheets for solar cells," *IEEE Trans. Electron. Dev.* **29**(2), 300–305 (1982).
5. M. Green, "Lambertian light trapping in textured solar cells and light-emitting diodes: Analytical solutions," *Prog. Photovolt. Res. Appl.* **10**(4), 235–241 (2002).
6. A. Bozzola, M. Liscidini, and L. C. Andreani, "Photonic light-trapping versus Lambertian limits in thin film silicon solar cells with 1D and 2D periodic patterns," *Opt. Express* **20**(S2 Suppl 2), A224–A244 (2012).
7. NREL, AM1.5G solar spectrum irradiance data: <http://rredc.nrel.gov/solar/spectra/am1.5>.
8. A. Luque, *Solar Cells and Optics for Photovoltaic Concentration* (Adam Hilger, Bristol, 1989).
9. R. Brendel, *Thin-Film Crystalline Silicon Solar Cells: Physics and Technology* (Wiley-VCH, 2003).
10. C. Battaglia, M. Boccard, F.-J. Haug, and C. Ballif, "Light trapping in solar cells: When does a Lambertian scatterer scatter Lambertianly?" *J. Appl. Phys.* **112**(9), 094504 (2012).
11. H. Sai, K. Saito, N. Hozuki, and M. Kondo, "Relationship between the cell thickness and the optimum period of textured back reflectors in thin-film microcrystalline silicon solar cells," *Appl. Phys. Lett.* **102**(5), 053509 (2013).
12. M. Berginski, J. Hüpkens, A. Gordijn, W. Reetz, T. Wätjen, B. Rech, and M. Wuttig, "Experimental studies and limitations of the light trapping and optical losses in microcrystalline silicon solar cells," *Sol. Energy Mater. Sol. Cells* **92**(9), 1037–1042 (2008).
13. V. Jovanov, U. Planchoke, P. Magnus, H. Stiebig, and D. Knipp, "Influence of back contact morphology on light trapping and plasmonic effects in microcrystalline silicon single junction and micromorph tandem solar cells," *Sol. Energy Mater. Sol. Cells* **110**, 49–57 (2013).
14. V. Depauw, X. Meng, O. El Daif, G. Gomard, L. Lalouat, E. Drouard, C. Trompoukis, A. Fave, C. Seassal, and I. Gordon, "Micrometer-Thin Crystalline-Silicon Solar Cells Integrating Numerically Optimized 2-D Photonic Crystals," *IEEE J Phot.*, in press (2013).

15. O. Isabella, A. Ingenito, D. Linssen, and M. Zeman, "Front/Rear Decoupled Texturing in Refractive and Diffractive Regimes for Ultra-Thin Silicon-Based Solar Cells," *Renewable Energy and the Environment*, OSA Technical Digest, paper PM4C.2 (2013).
16. E. R. Martins, J. Li, Y. Liu, V. Depauw, Z. Chen, J. Zhou, and T. F. Krauss, "Deterministic quasi-random nanostructures for photon control," *Nat Commun* **4**, 2665 (2013).
17. E. D. Palik, *Handbook of Optical Constants of Solids* (Academic, Orlando, 1985).
18. J. Zhao, A. Wang, P. P. Altermatt, S. R. Wenham, and M. A. Green, "24% Efficient per l silicon solar cell: Recent improvements in high efficiency silicon cell research," *Sol. Energy Mater. Sol. Cells* **41-42**, 87–99 (1996).
19. P. Campbell and M. A. Green, "Light trapping properties of pyramidally textured surfaces," *J. Appl. Phys.* **62**(1), 243 (1987).
20. P. Bermel, C. Luo, L. Zeng, L. C. Kimerling, and J. D. Joannopoulos, "Improving thin-film crystalline silicon solar cell efficiencies with photonic crystals," *Opt. Express* **15**(25), 16986–17000 (2007).
21. M. A. Green and M. J. Keevers, "Optical Properties of Intrinsic Silicon at 300 K," *Prog. Photovolt. Res. Appl.* **3**(3), 189–192 (1995).
22. J. Gjessing, A. S. Sudbø, and E. S. Marstein, "Comparison of periodic light-trapping structures in thin crystalline silicon solar cells," *J. Appl. Phys.* **110**(3), 033104 (2011).
23. X. Sheng, L. Z. Broderick, and L. C. Kimerling, "Photonic crystal structures for light trapping in thin-film Si solar cells: Modeling, process and optimizations," *Opt. Commun.* in press.
24. C. Trompoukis, O. El Daif, V. Depauw, I. Gordon, and J. Poortmans, "Photonic assisted light trapping integrated in ultrathin crystalline silicon solar cells by nanoimprint lithography," *Appl. Phys. Lett.* **101**(10), 103901 (2012).
25. F. Feldmann, M. Bivour, C. Reichel, M. Hermle, and S. W. Glunz, "A Passivated Rear Contact for High-Efficiency n-Type Si Solar Cells Enabling High Voc's and FF>82%," 28th EU PVSEC, 2CO.4.4 (2013).
26. L. Wang, J. Han, A. Lochtefeld, A. Geger, M. Carroll, D. Stryker, S. Bengtson, M. Curtin, H. Li, Y. Yao, D. Lin, J. Ji, A. J. Lennon, R. L. Opila, and A. Barnett, "16.8% Efficient Ultra-Thin Silicon Solar Cells on Steel," 28th EU PVSEC, 3DV.1.12 (2013).
27. J. H. Petermann, D. Zielke, J. Schmidt, F. Haase, E. G. Rojas, and R. Brendel, "19% efficient and 43µm thick crystalline Si solar cell from layer transfer using porous silicon," *Prog. Photovolt. Res. Appl.* **20**(1), 1–5 (2012).
28. J. Müller, B. Rech, J. Springer, and M. Vanecek, "TCO and light trapping in silicon thin film solar cells," *Sol. Energy* **77**(6), 917–930 (2004).
29. C. Haase and H. Stiebig, "Optical Properties of Thin-film Silicon Solar Cells with Grating Couplers," *Prog. Photovolt. Res. Appl.* **14**(7), 629–641 (2006).
30. S. E. Han and G. Chen, "Toward the Lambertian limit of light trapping in thin nanostructured silicon solar cells," *Nano Lett.* **10**(11), 4692–4696 (2010).
31. K. X. Wang, Z. Yu, V. Liu, Y. Cui, and S. Fan, "Absorption enhancement in ultrathin crystalline silicon solar cells with antireflection and light-trapping nanocone gratings," *Nano Lett.* **12**(3), 1616–1619 (2012).
32. S. B. Mallick, M. Agrawal, and P. Peumans, "Optimal light trapping in ultra-thin photonic crystal crystalline silicon solar cells," *Opt. Express* **18**(6), 5691–5706 (2010).
33. A. Mellor, I. Tobias, A. Marti, and A. Luque, "A numerical study of Bi-periodic binary diffraction gratings for solar cell applications," *Sol. Energy Mater. Sol. Cells* **95**(12), 3527–3535 (2011).
34. A. Mellor, H. Hauser, C. Wellens, J. Benick, J. Eisenlohr, M. Peters, A. Guttowski, I. Tobias, A. Martí, A. Luque, and B. Bläsi, "Nanoimprinted diffraction gratings for crystalline silicon solar cells: implementation, characterization and simulation," *Opt. Express* **21**(S2), A295–A304 (2013).
35. R. Dewan and D. Knipp, "Light trapping in thin-film silicon solar cells with integrated diffraction grating," *J. Appl. Phys.* **106**(7), 074901 (2009).
36. N. T. Fofang, T. S. Luk, M. Okandan, G. N. Nielson, and I. Brener, "Substrate-modified scattering properties of silicon nanostructures for solar energy applications," *Opt. Express* **21**(4), 4774–4782 (2013).
37. D. Lockau, T. Sontheimer, C. Becker, E. Rudigier-Voigt, F. Schmidt, and B. Rech, "Nanophotonic light trapping in 3-dimensional thin-film silicon architectures," *Opt. Express* **21**(S1), A42–A52 (2013).

## 1. Introduction

It is now well established that solar cells can make an important contribution to the renewable energy mix, with more than 100 GWp of capacity already installed [1]. The main impediment to further growth is the price/performance ratio; we need to reduce cost by using less material or increase efficiency by converting more of the incoming solar radiation into photocurrent, or, ideally, both. Using nanophotonic techniques, i.e. "light trapping", is a promising strategy to achieving these goals, and to enable the realisation of thinner solar cells with higher efficiency. Thinner solar cells may also benefit from higher open-circuit voltages due to reduced impact of bulk recombination: for crystalline silicon, for example, the limiting value increases from ca. 750 mV for a 300 µm thick cell to 830 mV for a 1 µm thick cell [2].

A large variety of light trapping structures has already been proposed and demonstrated in the literature; in order to identify the most promising structures, it is clearly important to describe their performance objectively and quantitatively. Typically, authors compare their proposed structures to an unstructured thin film and to an ideal Lambertian scatterer, the latter being a theoretical model derived from statistical ray optics considerations [3]. The Lambertian scatterer enhances the path length up to  $4n^2$  on average, where  $n$  stands for the refractive index of the absorbing material. The problem with this comparison is that it depends on the thickness of the absorber material and on the quality of the material itself. Further, the  $4n^2$  enhancement can be approached only in case of weak active absorption [4]: in other cases the active absorption has to be calculated by considering the attenuation of the single angular components of the scattered photon flux [4–6]. In the solar cells community it is well known that the Lambertian limit can be easily overcome at single wavelengths using different types of photonic approaches. Indeed, the main problem is to achieve enhancement at all (or at least most) wavelengths: for this reason we limited our analysis to works that report data calculated over the standard AM 1.5G spectrum [7]. In addition, authors often use different materials, substrates and different model assumptions to assess the performance of their respective structures. Experimental structures may also suffer from parasitic absorption in the oxide layers and in the electrodes, which theoretical models tend to ignore.

In order to provide a unified description of light trapping properties and to take this large variety of effects into account, we propose a new figure of merit to describe the light trapping performance, which we term the *light trapping efficiency (LTE)*. The LTE aims at assessing the performance of the nanostructure itself, irrespective of the material, fabrication method and technology used.

## 2. The format of the LTE figure of merit

The LTE uses the short-circuit current  $J_{SC}$  as a basis for describing the performance of a solar cell device;  $J_{SC}$  measures the number of electron-hole pairs generated by the incoming solar flux, which is the parameter that light trapping is aiming to increase.

We calculate the  $J_{SC}$  for the AM1.5 spectrum with the *global* irradiance of 100 mW/cm<sup>2</sup> on Earth [7] and assume an internal quantum efficiency of unity, as outlined in more detail below (see Eqs. (1)-(4)). Figure 1 shows the resulting values of  $J_{SC}$  as a function of thickness for three extreme cases; a)  $J_{LL}$ , for “Lambertian Limit”, assuming an ideal Lambertian scatterer with no external reflection losses (perfect anti-reflection coating) on the front surface and a perfect metal back-reflector, which yields the top (red dashed) curve; b)  $J_{MB}$ , for “Metal Back-reflector”, which assumes an unstructured, perfectly planar thin film with perfect anti-reflection coating and metal back-reflector, represented by the blue solid line, and c)  $J_{min}$ , the same as b) but without anti-reflection coating, which yields the bottom (black dotted) curve.

The  $J_{LL}$  of an ideal solar cell assumes an internal quantum efficiency of unity for all wavelengths  $\lambda$ , maximum pathlength enhancement due to scattering (see Appendix 2), a perfect anti-reflection coating and a perfect metal back-reflector:

$$J_{LL}(t_{tot}) = J_{sun} - \frac{e}{hc} \cdot \int_{300 \text{ nm}}^{1200 \text{ nm}} \frac{\lambda}{1 + \left(\frac{1 - T_r^2}{T_r^2}\right) \cdot n^2} \cdot \frac{dI_{sun}}{d\lambda} \cdot d\lambda. \quad (1)$$

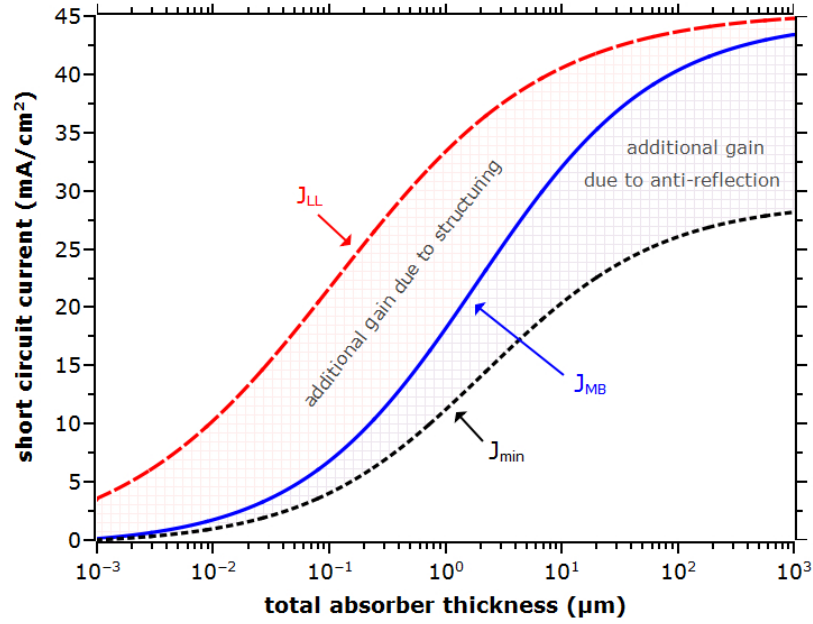


Fig. 1. Short-circuit currents as a function of the absorber thickness. The  $J_{MB}$  and  $J_{min}$  graphs correspond to currents generated by a double pass traversal of light in the absorber layer with (blue solid) and without (black dotted) perfect anti-reflection coating, respectively. The  $J_{LL}$  refers to devices textured with an ideal Lambertian scatterer and perfect anti-reflection coating (red-dashed line). All devices have a perfect mirror on the back.

$J_{LL}$  is always lower than the incident solar flux  $J_{sun}$  expressed as an electrical current of  $\sim 46 \text{ mA/cm}^2$  for the specified wavelength interval of the global AM1.5 solar spectrum  $dI_{sun}/d\lambda$ . The physical constants  $e$ ,  $h$  and  $c$  are the electron charge, Planck's constant and the velocity of light, respectively. In the case that light is fully randomized in a slab with thickness  $t_{tot}$ , its transmittance  $T_r$  can be expressed by an angle-averaged effective absorption coefficient  $\alpha_{eff}$  [5,8,9]:

$$T_r(t_{tot}) = e^{-(\alpha_{eff} \cdot t_{tot})} = 2 \cdot \int_0^{\pi/2} \cos \vartheta \cdot e^{-\alpha \cdot (t_{tot} / \cos \vartheta)} \cdot \sin \vartheta \, d\vartheta. \quad (2)$$

$T_r$  is always smaller or equal to the transmittance  $T_{sp}$  of a non-randomized single pass traversal, because for weakly absorbed light ( $\alpha t_{tot} \ll 1$ ) the enhancement factor describing randomisation alone, which can be expressed as  $(1-T_r)/(1-T_{sp})$ , is at best 2, while it is unity for strongly absorbed light ( $\alpha t_{tot} \gg 1$ ). Therefore,  $T_r$  measures Lambertian transmission through an absorbing layer and stands in contrast to the Lambertianity factor  $a$  from Battaglia et al. [10], which is independent of the material constant  $\alpha$ .

The  $J_{MB}$  corresponds to the short-circuit current generated by a double pass traversal of light in an ideal unstructured reference device, i.e. a solar cell with internal quantum efficiency equal to unity for all wavelengths  $\lambda$ , with a perfect anti-reflection coating and a perfect metal back-reflector:

$$J_{MB}(t_{tot}) = J_{sun} - \frac{e}{hc} \cdot \int_{300 \text{ nm}}^{1200 \text{ nm}} e^{-2\alpha \cdot t_{tot}} \cdot \lambda \frac{dI_{sun}}{d\lambda} \cdot d\lambda. \quad (3)$$

The difference  $J_{LL} - J_{MB}$  can then be understood as the maximum theoretical current gain due to light trapping. In addition, avoiding reflections is another major issue in solar cells and photonic patterns. To highlight the importance of anti-reflection, we consider the case of a slab without any coating, for which the short-circuit current  $J_{min}$  is calculated as follows:

$$J_{min}(t_{tot}) = J_{sun} - \frac{e}{hc} \cdot \int_{300 \text{ nm}}^{1200 \text{ nm}} \left( \frac{n-1}{n+1} \right)^2 \cdot e^{-2\alpha \cdot t_{tot}} \cdot \lambda \frac{dI_{sun}}{d\lambda} \cdot d\lambda. \quad (4)$$

When looking at literature proposals (c.f. section 3),  $J_{max}$  denotes the current of a proposed light trapping design, while we name with  $J_{ref}$  the short circuit current of its (unpatterned) reference device. Real solar cells may not achieve the theoretical values  $J_{LL}$  or  $J_{MB}$ , respectively, because of material imperfections, parasitic absorption or imperfect anti-reflection coating. The term  $J_{max} - J_{ref}$  therefore represents the improvement in current achieved by the real structure.

The LTE then compares the total current gain  $J_{max} - J_{ref}$  achieved by the real structure to the theoretical maximum current gain of the *ideal* Lambertian scatterer  $J_{LL} - J_{MB}$ , so our expression for the light trapping efficiency (LTE) takes the format

$$LTE = \frac{J_{max} - J_{ref}}{J_{LL} - J_{MB}}. \quad (5)$$

We make the following comments and assumptions:

1. Light trapping for photovoltaic applications aims to increase the absorption over the *full wavelength range* of the global solar spectrum (from 300 nm up to the wavelength bandgap). All currents therefore refer to the full AM1.5G standard spectrum [7].
2. All practical solar cells use a *back-reflector* for doubling the optical path length and for increasing the absorption probability of light. Therefore,  $J_{LL}$  and  $J_{MB}$  represent ideal solar cells with mirrors that exhibit no parasitic absorption, while  $J_{max}$  and  $J_{ref}$  include the properties of real mirrors.
3. We note that the LTE has the same format as the efficiency  $\eta$  of a Carnot engine:

$$\eta_{Carnot} = \frac{T_{abs} - T_o}{T_{abs} - 0}. \quad (6)$$

where the temperature difference of an absorber and its surrounding air (nominator in Eq. (6)) is compared to the maximum possible temperature difference (denominator in Eq. (6)).

4. Once the optimized  $J_{ref}$  is found, the *same anti-reflection coating and back-reflector* are applied to the structured solar cell device. In doing so,  $J_{max}$  purely reflects the benefits of texturing the absorber material.
5. Our literature analysis is applied to crystalline silicon (c-Si). Since the absorber material used for  $J_{ref}$  *also defines the values of  $J_{LL}$  and  $J_{MB}$* , the LTE remains applicable to any other technology or material. The LTE figure of merit is thus only limited by the availability of material parameters.
6. Previous results indicate that the number of photogenerated electron-hole pairs is often found to be lower than the total measured absorption [11], which points to the presence of parasitic absorption. The short-circuit currents  $J_{max}$  and  $J_{ref}$  can therefore *not be*

determined by the total simulated or measured absorption characteristic, but must refer to the sole active absorption, as already pointed out by several authors [12–14].

- To allow easier comparison of different approaches, we define the LTE for the total thickness of the absorber material. Other authors often refer to the effective thickness  $t_{eff}$ , which is a useful concept for comparing light trapping structures in terms of their material budget. However, the performance of a scatterer depends not only on the volume of the absorber material or on the geometry of the structures: the volume of material between the structures plays an equally important role as the scattering material itself (see Fig. 2). After all, scattering only happens at interfaces between materials of different refractive index, not in the homogenous material itself.

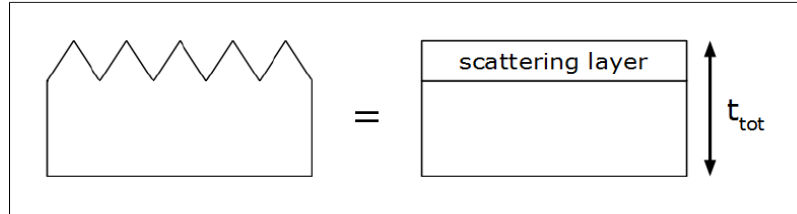


Fig. 2. The performance of a scatterer relies on the refractive index contrast and thus on the materials between the structures. Therefore, the LTE is defined for the total thickness  $t_{tot}$  of the absorber material that includes the scattering layer.

### 3. Results

We applied the LTE defined in Eq. (5) to several c-Si solar cells found in the literature. While the majority of proposals are numerical simulations, some experimental results of hydrogenated microcrystalline silicon ( $\mu\text{-Si:H}$ ) devices are included in our study as well. However, since the material properties of  $\mu\text{-Si:H}$  depend on both the growth conditions and the substrate layer, the LTEs of these structures are qualitatively assessed with the optical constants of c-Si. Figure 3 gives a review of the assessed structures, while the corresponding short-circuit currents are listed in Table 1, Table 2, and Table 3.

When the reference structure was not provided for the total thickness, we decided to use  $J_{MB}$  as the reference in order to highlight light trapping performances.

### 4. Conclusions

We have introduced a new figure of merit to quantify the benefit of nanostructures for light trapping in solar cells, termed the light trapping efficiency (LTE). The LTE uses the short circuit current to assess the performance of a given light trapping design and compares it to an ideal Lambertian scatterer. The main difficulty in compiling a comprehensive overview of literature values is the large variety of parameters reported by authors, so we appeal to the community to become more consistent in how it reports efficiency enhancements and light trapping performance; we hope our work acts as an inspiration in this regard. Similarly, we are not able to identify the “best” light trapping structure realised thus far, because it may be based on amorphous silicon or some other material without providing the relevant material properties. The fact that the performance of theoretical structures is significantly above that of experimental ones points to the need of theoretical studies to take “real” effects such as parasitic absorption better into account. In principle, the light trapping problem appears close to being solved, since we have identified a number of structures close to the ideal performance of  $\text{LTE} = 1$ . Naturally, demonstrating such high light trapping performance in real devices is another matter, which needs to be tackled next. Finally, the high performance of [15] and [16] highlights the need to achieve both high performance in light trapping and in antireflection, ideally together.

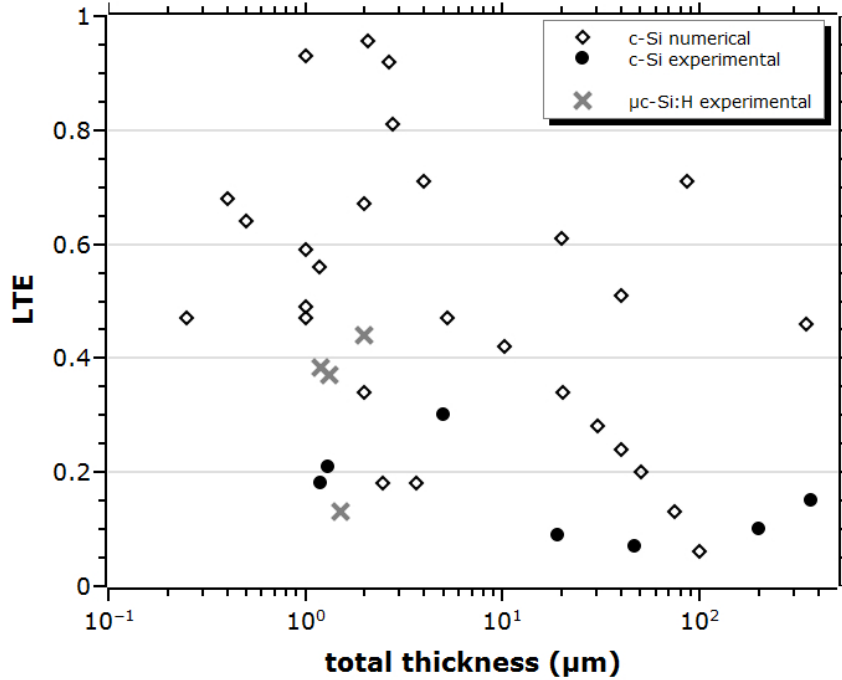


Fig. 3. The calculated light trapping efficiency (LTE) of proposed c-Si structures in literature. All  $\mu\text{c-Si:H}$  data points were also qualitatively assessed with the optical constants of c-Si [17]. While the LTE is, in principle, independent of absorber thickness, we note that the highest performing structures operate in the  $1\mu\text{m} - 5\mu\text{m}$  range, which we believe is motivated by the fact that the benefit of light trapping is maximum in this thickness range. We also note that solar cells with the highest efficiency (e.g. the PERL cell of [18]) are not necessarily the best light trapping structures, which highlights the difference between the LTE and the absolute efficiency as well as the importance of anti-reflection coating, as already shown in Fig. 1.

**Table 1. Experimental structures using c-Si.**

| LTE  | thickness ( $\mu\text{m}$ ) | $J_{max}$ | $J_{ref}$ | $J_{LL}$ | $J_{MB}$ | reference |
|------|-----------------------------|-----------|-----------|----------|----------|-----------|
| 0.30 | 5.00                        | 17.5      | 14.7      | 38.3     | 29.0     | [23]      |
| 0.21 | 1.30                        | 15.5      | 12.5      | 34.4     | 20.1     | [24]      |
| 0.19 | 1.48                        | 15.4      | 12.8      | 34.8     | 20.9     | [14]      |
| 0.15 | 370.0                       | 40.9      | 40.5      | 44.5     | 41.8     | [18]      |
| 0.10 | 200.0                       | 41.0      |           | 44.1     | 40.6     | [25]      |
| 0.09 | 19.00                       | 35.5      |           | 41.1     | 35.0     | [26]      |
| 0.07 | 47.00                       | 37.8      |           | 42.6     | 37.4     | [27]      |

**Table 2. Experimental structures using  $\mu\text{c-Si:H}$  (qualitatively assessed with c-Si [17]).**

| LTE  | thickness ( $\mu\text{m}$ ) | $J_{max}$ | $J_{ref}$ | $J_{LL}$ | $J_{MB}$ | reference |
|------|-----------------------------|-----------|-----------|----------|----------|-----------|
| 0.44 | 2.00                        | 28.7      |           | 35.8     | 23.1     | [11]      |
| 0.38 | 1.20                        | 20.8      | 15.3      | 34.4     | 20.1     | [28]      |
| 0.37 | 1.33                        | 17.7      | 12.4      | 34.5     | 20.2     | [29]      |
| 0.13 | 1.50                        | 9.9       | 8.1       | 34.9     | 21.1     | [23]      |

**Table 3. Numerical structures using c-Si (considering the best proposal in each reference).**

| LTE  | thickness ( $\mu\text{m}$ ) | $J_{max}$ | $J_{ref}$ | $J_{LL}$ | $J_{MB}$ | reference |
|------|-----------------------------|-----------|-----------|----------|----------|-----------|
| 0.96 | 2.73                        | 33.9      | 23.2      | 36.2     | 25.0     | [15]      |
| 0.93 | 1.00                        | 29.1      | 15.0      | 33.5     | 18.3     | [16]      |
| 0.92 | 2.65                        | 35.7      |           | 36.6     | 25.0     | [30]      |
| 0.84 | 20.00                       | 37.3      | 31.3      | 41.1     | 34.0     | [22]      |
| 0.81 | 2.78                        | 34.6      |           | 36.8     | 25.3     | [31]      |
| 0.71 | 4.00                        | 32.0      | 24.8      | 37.6     | 27.6     | [6]       |
| 0.71 | 86.67                       | 42.0      |           | 43.3     | 38.8     | [19]      |
| 0.68 | 0.40                        | 21.8      | 10.3      | 29.6     | 12.5     | [32]      |
| 0.67 | 2.00                        | 29.4      | 21.0      | 35.7     | 23.0     | [6]       |
| 0.64 | 0.50                        | 21.5      | 12.0      | 28.7     | 13.8     | [6]       |
| 0.59 | 1.00                        | 25.4      | 16.5      | 33.3     | 18.3     | [6]       |
| 0.56 | 1.19                        | 27.6      | 19.4      | 34.1     | 19.4     | [33]      |
| 0.51 | 40.00                       | 36.4      | 33.7      | 42.3     | 37.0     | [34]      |
| 0.47 | 5.22                        | 33.6      |           | 38.4     | 29.2     | [33]      |
| 0.47 | 0.25                        | 16.4      | 8.3       | 27.2     | 9.9      | [6]       |
| 0.47 | 1.00                        | 24.2      | 17.1      | 33.5     | 18.3     | [35]      |
| 0.46 | 346.67                      | 43.0      |           | 44.5     | 41.7     | [19]      |
| 0.42 | 10.23                       | 35.7      |           | 39.9     | 32.6     | [33]      |
| 0.34 | 2.00                        | 23.6      | 19.3      | 35.8     | 23.1     | [20]      |
| 0.34 | 20.26                       | 37.2      |           | 41.2     | 35.2     | [33]      |
| 0.28 | 30.24                       | 37.9      |           | 41.9     | 36.3     | [33]      |
| 0.24 | 40.24                       | 38.3      |           | 42.3     | 37.1     | [33]      |
| 0.20 | 50.24                       | 38.6      |           | 42.7     | 37.6     | [33]      |
| 0.18 | 2.48                        | 26.7      |           | 36.5     | 24.5     | [36]      |
| 0.18 | 3.65                        | 29.0      |           | 37.5     | 27.1     | [37]      |
| 0.13 | 75.27                       | 39.1      |           | 43.2     | 38.5     | [33]      |
| 0.06 | 100.27                      | 39.4      |           | 43.5     | 39.2     | [33]      |

## Appendix 1

We like to add some specific comments to the quoted numbers and the selection of the papers.

Since the LTE is defined for the total thickness, we always recalculated  $J_{LL}$  and  $J_{MB}$  when authors referred to the effective thickness, e.g [19].

If the short-circuit currents were not quoted but the numerical absorption spectra provided [20], we used the free software tool Plot Digitizer from sourceforge.net in order to calculate the LTE of the structure. Since we always assumed an internal quantum efficiency equal to unity in numerical proposals, we excluded spectra where we suspected a parasitic influence. The criterion here was a high absorption near the wavelength bandgap of silicon: for a 300  $\mu\text{m}$  thick layer, it takes a single-pass traversal to absorb 10% of the light, while in a 1  $\mu\text{m}$  thick slab 20% would already be absorbed by a 99% reflective metal (assuming  $2n^2$  “bounces” against the mirror).

Theoretical studies often use the optical constants provided by [17] or [21]. We tried to take this into account for the LTE. However, if we found  $J_{ref}$  too close to the current of a single-pass traversal, we recalculated the reference with the same optical constants, e.g [22].



## Appendix 2

The absorption enhancement of a thin-film with a Lambertian scattering layer was independently derived by [5] and [9]. The same equations can be derived in a very intuitive way considering the attenuation of a propagating incoherent light ray in a lossy waveguide.

Our ansatz is schematically shown in Fig. 4, where we first distinguish between the top and bottom angle-averaged transmission coefficients  $T^+$  and  $T^-$ . Since the Lambertian Scatterer is situated on the backside, the first traversal will be a single-pass transmission  $T_{sp}$  which is greater than  $T^+$ . The effective back- and front reflectance,  $R_b$  and  $R_f$ , are then determined by the amount of light leaving the absorber into the adjacent layers.

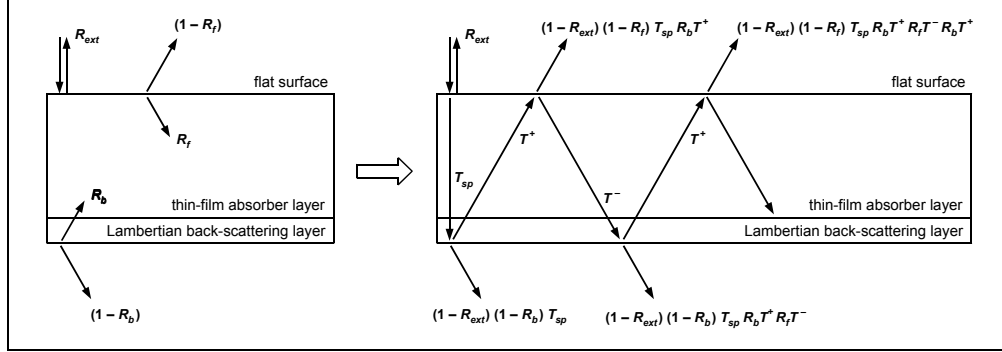


Fig. 4. When randomization of light at the scattering layer allows to neglect coherent effects, the propagation of an average light ray in a lossy waveguide is described by the external reflection  $R_{ext}$ , the internal effective reflectances  $R_f$  and  $R_b$  and the attenuated transmissions  $T^+$  and  $T^-$  respective to a single-pass traversal  $T_{sp}$ .

The absorption can now be calculated via

$$\begin{aligned}
 A &= 1 - R - T \\
 &= 1 - \left[ R_{ext} + (1 - R_{ext})(1 - R_f)R_b T_{sp} T^+ \cdot \sum_{m=0}^{\infty} (R_b R_f T^- T^+)^m \right] - \\
 &\quad - \left[ (1 - R_{ext})(1 - R_b) T_{sp} \cdot \sum_{m=0}^{\infty} (R_b R_f T^- T^+)^m \right] \\
 &= (1 - R_{ext}) \cdot \frac{(1 - T_{sp}) + R_b T_{sp} \cdot [(1 - T^+) + R_f T^+ \cdot (1 - T^- / T_{sp})]}{1 - R_b R_f T^- T^+}. \quad (7)
 \end{aligned}$$

When the Lambertian Scatterer is situated on top of the device, i.e.  $T \rightarrow T^-$ , and we assume that light is fully randomized,  $T_r = T^+ \approx T^-$ , we exactly find the previous derived equation from Brendel [9]:

$$A = (1 - R_{ext}) \cdot \frac{(1 - T_r)(1 + R_b T_r)}{1 - R_b R_f T_r^2}. \quad (8)$$

While M. Green [5] distinguishes between  $T^+$  and  $T^-$ , we did not find any discrepancy in the outcoming result by using the assumption of  $T^+ \approx T^-$ . This also means that the absorption does not differ by much for dual or top Lambertian textures.

If the back-reflector is a perfect mirror, the front surface perfect anti-reflective and the incident medium air, we have  $R_b = 1$  and  $R_f = 1 - 1/n^2$  leading to the absorption used in Eq. (1):

$$A = \frac{1 - T_r^2 + \frac{T_r^2}{n^2} - \frac{T_r^2}{n^2}}{1 - \left(1 - \frac{1}{n^2}\right) \cdot T_r^2} = 1 - \frac{1}{1 + \left(\frac{1 - T_r^2}{T_r^2}\right) \cdot n^2}. \quad (9)$$

### Acknowledgments

We wish to thank Daan Stellinga as well as Ken Xingze Wang of Stanford University and Olindo Isabella of Delft University for helpful discussions. This work was supported by the EU through Marie Curie Action FP7-PEOPLE-2010-ITN Project No. 264687 "PROPHET".